ION MASS SPECTROMETRY : A NEW METHOD FOR ATMOSPHERIC TRACE GAS ANALYSIS

E. ARIJS, D. NEVEJANS and J. INGELS
Belgisch Instituut voor Ruimte-Aëronomie
Ringlaan 3, 1180 Brussel

1. INTRODUCTION

Apart from the well known major components (such as nitrogen, oxygen, water vapour, carbon dioxide and the noble gases), the atmosphere of the Earth contains a number of gaseous compounds (e.g. nitrogen oxides, methane, a.s.o), the total mixing ratio of which is of the order of about 700 ppm and which are mostly referred to as trace gases.

Whereas the mixing ratio of the major gases except water vapour, is kept constant by turbulence up to about 100 km (region of the atmosphere called therefore "HOMOSPHERE"), the mixing ratio of some of the trace gases varies with altitude due to a combination of transport phenomena, chemical reactions and photodissociation. A typical example is the mixing ratio profile of ozone, one of the most important trace gases in view of its filtering effect of the harmful UV light.

It has been discovered that trace gases down to the ppb (or even ppt) level can play an important role in the physical chemistry of the gaseous mantle of our planet. Typical examples are :

- the importance of nitrogen oxides or chlorine compounds in the "STRATOSPHERE" (the region of the atmosphere where the temperature gradient versus altitude is positive, at our latitude between 12 and 50 km) in the catalytic destruction of ozone, which has become topical in recent years, due to the discovery of the ozone hole over Antarctica.
- the role played by sulfur compounds, either naturally emitted by episodic volcanic eruptions or man made by industrial activities, in the formation of aerosols and their possible impact on our climate.

One of the primary concerns of scientists active in the field of aeronomy has therefore always been to design and apply experimental methods to measure trace gases in our atmosphere. In this respect, much attention has been paid to the stratosphere where the ozone layer resides and which is rather easily accessible with balloon-borne instruments.

Presently, a wide variety of trace gas measuring techniques has been developed based on remote sensing (mostly optical) methods from ground level, balloons and satellites; as well as on in-situ measurement methods such as grab- or cryosampling of gases, followed by laboratory analysis with classical methods such as gas chromatography.

BELVAC NEWS, 4, Nr. 1, 1988, 5-34

Recently however, it has been recognized that ion mass spectrometry which was originally developed to study the identity of natural ions, formed by galactic cosmic radiation and subsequent ion-molecule reactions, may turn out to become a powerful technique for trace gas analysis.

2. THE EXPERIMENTAL METHOD

2.1. Historical background and original objectives

As a result of the energetic radiation input to the Earth's atmosphere (high energy particles from the solar wind, X-rays and UV-radiation from the sun and cosmic rays), part of it is ionized which results in a rarefied plasma surrounding our planet, called the "IONOSPHERE". At altitudes where the density is low enough to avoid electron attachment processes (roughly about 60 km), this plasma consists of positive ions and electrons. Based on the average electron density profile, the ionosphere has been devided into three characteristic layers, as shown in figure 1. The D-region (60 to 85 km) is mainly produced by the ionization of nitric oxide by solar Lyman-α radiation (UV light at 121.6 nm), and to a lesser extent by high energy cosmic ray ionization of nitrogen and oxygen. The E-region, located between 85 and 130 km, results from ionization of nitrogen and oxygen by X-rays and Lyman-radiation. The F-region (above 130 km), subdivided into F1- and F2-layers, is produced by photoionization of nitrogen and atomic oxygen by extreme U.V. radiation.

Above the F-layer, which predominantly contains atomic oxygen ions, the electron density decreases rapidly. At higher altitudes, helium and hydrogen ions start to prevail and the Earth's magnetic field begins to play an important role in the behaviour of the charged particles. This upper region of the atmosphere is therefore called the "MAGNETOSPHERE".

The D, E and F-layers of the ionosphere play an important role in the reflection or propagation of radiowaves and have therefore extensively been studied by ground based radio-sonde techniques in relation with telecommunication problems.

Radiosonde studies however, only give information about electron densities and do not tell us anything about the nature of the ions present in the ionosphere. Therefore, several experimental studies have been performed with rocket- or satellite-borne mass spectrometers to reveal the ion composition [1, 2].

It turned out that in the F- and E- layers, the major ions where O_2^+ and NO^+, formed either through direct ionization processes or through the ion-molecule reactions :

$$N_2^+ + O \rightarrow NO^+ + N \qquad (1)$$
$$\rightarrow O^+ + N_2$$

$$O^+ + N_2 \rightarrow NO^+ + N \qquad (2)$$

$$O^+ + O_2 \rightarrow O_2^+ + O \qquad (3)$$

and to a lesser extent

$$N_2^+ + O_2 \rightarrow O_2^+ + N_2 \qquad (4)$$

For the D-region however, the situation is somewhat more complicated. It has been suggested by Nicolet that the presence of the D-region was due to the photoionization of nitric oxide by solar Lyman α radiation. As a result of a theoretical study by Nicolet and Aikin [3], it was expected that the major ions in the D-region would be O_2^+ and NO^+. However, the pioneering work of Narcissi and his group [4] with rocket-borne mass spectrometers showed that apart from those primary ions a number of unexpected ions were present, which were identified as proton hydrates (PH), i.e. ions of the form $H^+(H_2O)_n$. Considerable laboratory and theoretical work as well as numerous in-situ measurements have been necessary to explain the conversion of the primary O_2^+ and NO^+ ions into the terminal PH [5-8]. In fact, a rather complicated scheme of ion-molecule reactions had to be proposed to explain this conversion. A detailed description of this scheme is beyond the scope of this paper, but excellent reviews can be found in the literature [9].

Whereas radiosonde measurements had shown the near absence of electrons below about 70 km, the observation of positive ions and the electro-neutrality condition requires the presence of negative ions in the D-region. These negative ions are formed by attachment of the free electrons to oxygen, followed by a set of ion-molecule reactions converting these "primary" ions into "terminal" ions, the nature of which will depend strongly on the nature of trace gases present in the atmosphere. The reaction scheme involved here has been derived primarely from laboratory work and confirmed by in-situ measurements with rocket-borne mass spectrometers [7, 9, 11]. We will not go into the details of it here, especially because it is very similar to the one applicable in the lower stratosphere, which will be reviewed hereafter.

The main source of ionization in the altitude region 10-50 km is cosmic radiation. This non selective ionizing radiation primarely yields N_2^+ and O_2^+, as well as electrons as primary charged particles. The electrons however attach very rapidly to molecular oxygen and the resulting rarefied plasma consists of positive and negative ions. As a result of the very low ionization rate Q (about 5 ion pairs/cc at 25 km) [12] and the value of the ion-ion recombination coefficient α (about 5×10^{-7} cm^3 s^{-1} at 25 km) [13], the ion number density is very low. In fact an application of the simple steady state equation :

$$Q = \alpha n^2 \qquad (5)$$

with $Q = 5$ cm^{-3} s^{-1} and $\alpha = 5 \times 10^{-7}$ cm^3 at 25 km, yields $n \simeq 3200$ cm^{-3}. Thus very low ion concentrations are expected in the stratosphere.

The corresponding ion lifetime being very long ($\tau = 1/\alpha n$), the ions make many collisions with neutrals before disappearing through recombination. Some of these collisions give rise to ion-molecule reactions changing the nature of the ions.

Concerning the ion composition of the atmosphere below 60 km, the only information available before 1977 was coming from laboratory work, giving an insight in the possible ion-molecule reactions involved, or from theoretical studies, resulting in models extending the results obtained for the D-region. The reaction schemes for the ion chemistry in the lower stratosphere as proposed before 1977 are shown in figures 2 and 3.

As in the D-region the expected "terminal" positive ions were again PH. However it was realized at that time that if a trace gas "A", with a higher proton affinity than that of water, would exist, the reaction scheme shown in figure 2 could be extended and other terminal ions than PH might exist. The terminal negative ions expected in the lower stratosphere are shown on the last line of figure 3. It should be pointed out that apart from the terminal ions, shown in double rectangles in figures 2 and 3, no other ions would be measurable with a mass spectrometer. The intermediate ion species, such as O_4^+ and O_4^- e.g., have a very short lifetime and disappear practically immediately.

Apart from the models, summarized in figures 2 and 3, no data were available about the stratospheric ion composition up to 1977. One of the initial objectives of a project called "ION", at the Belgian Institute for Space Aeronomy therefore was to build a mass spectrometer capable of investigating the ion composition of the lower atmosphere. This instrument, as well as the results obtained with it, will be described in the following sections. It will then be shown that the measurement of the stratospheric ion composition can lead to a new detection method of some trace gases and the future possible perspectives will be discussed.

2.2. INSTRUMENT DESCRIPTION AND EXPERIMENTAL METHOD

2.2.1. Measurement problems and instrument design

The experimental problem, we are facing is to sample ions from a gas at a rather high pressure (several millibars) and to bring them into a mass spectrometer which is functioning at high vacuum. This problem, which can be overcome in the laboratory by differential pumping with high speed vacuum pumps, is far from simple if we take into account that the instrument has to be limited in weight because it has to be taken into the atmosphere with a balloon. Fortunately, stratospheric ballooning techniques allow us to carry weights as high as several hundreds of kg (at the start of the project, in 1972, this weight was limited to 350 kg in Europe). Nevertheless it should be taken into account that the instrument must be independently powered by batteries and that it should contain adequate electronics. Furthermore, appropriate provisions should be made to recover the instrument undamaged after this balloon flight, which means mounting it in a mechanical support structure capable of taking the landing shock. All this means extra but necessary weight.

Through a series of extensive laboratory tests and three technological balloon flights, a solution for all these problems has evolved which is shown in figure 4. This figure represents a schematic overview of a typical ION balloon gondola element. It contains four major parts :

A. The high vacuum part consisting of a high speed liquid helium cryopump in which the mass spectrometer is built;

B. A special opening device, which remains closed as long as the instrument is not at the altitudes, where the measurements should begin and which can be opened by remote control from the ground station;

C. The electronic compartment, i.e. a light weight aluminium cylinder, sealed with a large aluminium flange on which the cryopump is mounted. This vessel is pressurized with dry air at one atmosphere to avoid breakdown problems in some of the electronic power supplies delivering high voltages. It contains all of the electronic modules, mounted on several platforms parallel to the large sealing flange. On the latter, hermetically sealed connectors are provided for telemetry, telecommand and testing the instrument;

D. The support structure and crash pad, which are made completely out of metal (aluminium) to avoid charging-up problems. Its geometry is adaptable to specific needs, such as flying multiple experiment payloads.

A complete instrument module as shown in figure 4, normally weighs about 125 kg. A gondola used for flight normally consists of 2 such modules, packed together and completed with a telemetry package and some additional small instruments to measure simultaneously ambient pressure and temperature.. Progress in ballooning techniques have in the meantime allowed higher payload weights and occasionally three modules have been combined in one gondola. In view of contamination problems heavily outgassing materials are avoided as much as possible for the construction of the payload.

2.2.2. Detailed instrument description

The high vacuum part of a typical payload as developed at our institute is pictured in figure 5. It consists of a high speed cryopump, a sampling hole, a remote opening device and a quadrupole mass filter with an ion focussing device and an ion detector.

On the downward looking large flange of the cryopump, a smaller flange is mounted, electrically insulated from the pump body. This "sampling" flange can by remote control, be put on different voltages (draw-in potential) to attract ions. Its central part is reduced to a thickness of about 0.1 mm and a small hole with a diameter of about 0.2 mm is drilled in its center. Prior to the balloon launching, this sampling aperture is covered with a polyimide plunger. Once the balloon has reached the desired working altitude (between 20 and 45 km), an opening device controlled by telecommand is activated and the plunger is removed, thus allowing the atmospheric air to flow into the instrument. The neutral gas molecules are scattered on metallic parts inside the instrument and absorbed on the cold walls of the liquid helium container. The ions however are focussed by an ion lens into the quadrupole, where they are filtered according to their mass-to-charge ratio. Each ion hitting the electron multiplier gives rise to a signal count, which is treated by a pulse discriminator and counter and routed to an on board microprocessor, which builds up the ion spectra sent to the ground station by telemetry.

To prevent scattering of the sampled ions by background gas particles, to obtain proper functioning of the quadrupole filter and to avoid voltage breakdown in the electron multiplier a vacuum of less than 10^{-4} mbar is required in the instrument. The outside pressure ranging from about 1 to 100 mbar, one of the basic problems was to design a cryopump with a high pumping speed and a long standing time (a balloon flight can take as long as 12 hours, including launching and recovery). To overcome this difficulty, a liquid helium cryopump was developed in collaboration with Leybold-Heraeus (Köln, B.R.D.), which has been discussed in detail elsewhere [14, 15] and will therefore only be described briefly here.

The body of the liquid helium cooled cryopump is made of stainless steel and all flanges are sealed with copper or polyimide (Vespel) O-rings. Thermal insulation of the helium bath is achieved by aluminized glass tissue super-insulation and two copper radiation shields, which are cooled by the evaporating cold helium gas passing through a copper spiral attached to these shields. An inner blackened chevron baffle protects the helium bath from the thermal radiation of the ion lens, quadrupole and ion detector. With these precautions, a standing time of about 12 hours has been achieved with a helium reservoir of 2.3 liters.

Figure 6 gives a more realistic view of the experimental set-up. In the present configuration, the ion lens and the quadrupole filter are mounted rigidly on the sampling flange to avoid alignment problems.

Various quadrupoles have been used in previous flights. Most frequently however, a filter with a rod radius of 6.3 mm and a rod length of 120 mm was employed. With a specially designed power supply (powered from lithium batteries), a mass range up to 330 amu could easily be achieved.

In our set-up mostly used, the ion focussing device consists of a single cylindrical lens element put in front of a commercially available ionizer (Finnigan). It should be stressed that this ionizer was only used as a lens (putting the different elements of it at the appropriate voltages). However the filament of it can be operated by remote control, thus allowing a check of the instrument or in-flight calibration by enhancing the ion content of the sampled air. The electron multiplier used is a Spiraltron type SEM 4219.

In the pressurized vessel mounted above the cryopump the different electronic modules described in detail before [15], are housed. A block diagram of the on-board electronics is shown in figure 7. It contains the ion lens supply, a high voltage power supply for the spiraltron and a power supply for the Penning gauge, which measures the vacuum in the cryopump during flight.

The quadrupole power supply produces the DC and RF voltages required to drive the quadrupole mass filter. It is designed so that the DC and RF can be controlled independently, allowing a great variety of operating modes. With a quadrupole having a rod diameter of 6.3 mm, the present unit covers a mass range from 0 to 330 amu at high resolution, using a 1500 V peak-to-peak RF excitation at 2 MHz.

A microprocessor (INTEL 8080) based control and data management unit has been included in the instrument to enhance the performances [16]. This unit performs the following main tasks :

- it controls the polarity of the ion lens and the spiraltron high voltage,
- it determines automatically the optimum draw-in potential for the sampling flange,
- it produces the ramping voltage to drive the quadrupole power supply,
- it counts the pulses leaving the pulse buffer, following the spiraltron and stores the values in a spectrum memory,
- it acquires important parameters of the ambient, such as temperature and pressure,
- it does remote control interpretation and organizes transmission of the spectrum and housekeeping data in analog and digital (PCM) format.

All of these duties are governed by software stored on-board in a non-volatile memory.

One of the key features of this unit is that, by the combination of a set of simple telecommand signals, it allows the choice of different measurement programs, such as : selection of positive and negative ion mode, selection of mass range and resolution and selection of a set of pre-programmed measurement tasks.

The described assembly of electronic modules is connected to an independent telecommand-telemetry system (SITTEL TM-TC), which is delivered by the balloon launching organization (CNES, Centre National d'Etudes Spatiales, Division Ballons, France).

3. EXPERIMENTAL RESULTS

Since 1977, several balloon flights have been performed with ion mass spectrometers to determine the natural ion composition in the stratosphere. All of these flights were realized in Europe, at the launching bases of the CNES in Aire-sur-l'Adour or Gap-Tallard in Southern France. Only two groups have been successfully active in this field, the group of the Belgian Institute for Space Aeronomy (further on abbreviated as BISA) and the one of the Max-Planck-Institut für Kernphysik of Heidelberg (further on called MPIH). The progress in ballooning techniques (valve controlled balloons, allowing slow descent of the balloon from ceiling altitude on, and high volume carriers, up to 1.000.000 cubic meters) have allowed the probing of an atmospheric layer from roughly 20 to 45 km altitude. The results of most of these measurements have been described extensively in the literature (see review papers by Arnold [17] and Arijs [18, 19]). Therefore, we will only give a concise description of it here and focus on the implications of the data for trace gas detection.

3.1. Positive ions

A typical positive ion spectrum obtained at 35 km altitude is shown in figure 8. This spectrum, which was taken at moderate resolution, clearly shows the major positive ions observed throughout the whole stratosphere. In fact figure 8 represents the very first spectrum of positive ions obtained in the stratosphere with a balloon-borne instrument [20]. The major positive ions and their identification are summarized in table 1. The mass determinations have been confirmed later on by higher resolution data of our group [21] and results of the MPIH group [22, 23].

As expected from previous modelling work, one major ion family consists of the proton hydrates (PH), but apart from this, another group is found which has been called the non proton hydrates (NPH) and the ions of which can be represented by the formula $H^+X_\ell(H_2O)_m$. The presence of these ions can be explained by ion-molecule reactions of the type :

$$H^+X_\ell(H_2O)_m + X \rightarrow H^+X_{\ell+1}(H_2O)_{m-1} + H_2O \qquad (5)$$

$$H^+X_\ell(H_2O)_m + H_2O + M \rightarrow H^+X_\ell(H_2O)_{m+1} + M \qquad (6)$$

and

$$H^+X_\ell(H_2O)_m + X + M \rightarrow H^+X_{\ell+1}(H_2O)_m + M \qquad (7)$$

where M is a third body reaction partner (typically oxygen or nitrogen), which does not participate in the reaction, but carries away the excess energy. (Reaction (5) explains the conversion of PH to NPH for $\ell = o$). The molecule X should have mass 41 amu to fit into the observed mass pattern. Furthermore, X should also have a proton affinity larger than that of water in order to make switching reactions of type (5) possible.

At present, the most likely candidate for this molecule seems to be acetonitrile according to laboratory work and in-situ experiments [24-27].

If we accept the formation mechanism as proposed by reactions (5), (6) and (7) for the NPH and assume that the NPH disappear by ion-ion recombination, we can write the steady state equation :

$$k\,[X]\,[PH] = \alpha\,[NPH]\,[n^-]$$

where k is the reaction rate coefficient for switching of type (5), α is the ion-ion recombination coefficient and $[n^-]$ represent the total negative ion number density, which according to the charge neutrality equals the total positive ion number density (square brackets in equation 8 represent total number densities).

The reaction rate coefficient k and the recombination coefficient have been measured in the laboratory [24] and $[n^-]$ can be estimated from previous parametrization studies based on total ion density in-situ measurements [28]. Therefore, the number density and consequently the mixing ratio of acetonitrile can be deduced from the observed ratio of NPH/PH in a mass spectrum if we assume that the peak height in the spectra are representative for the ion densities.

Figure 9 represents the mixing ratio profile of CH_3CN (acetonitrile) as derived with formula (8) for the different balloon flights performed by our group and the MPIH group. The ratio R of NPH-to-PH abundances was derived directly from the spectra. For the ion-ion recombination coefficient, a value was calculated with the expression :

$$\alpha = 6 \times 10^{-8} (300/T)^{1/2} + 1.25 \times 10^{-25} [M] (300/T)^{4} \qquad (9)$$

where [M] is the total neutral density and T temperature. This expression results in values of α which are in reasonable agreement [29] with laboratory data [24], theoretical values [30] and recent in-situ measurements [31].

Using this value of α, the negative ion number density $[n^-]$ was derived from

$$[n^+] = [n^-] = (Q/\alpha)^{1/2} \qquad (10)$$

where Q was calculated according to a parametrization developed by Heaps [32].

The mixing ratio profile of acetonitrile as shown in figure 9 suggests that we are dealing with a gas which is released at the Earth's surface, diffuses into the atmosphere and is destroyed on its way up. Additional evidence for this was given by the measurements of Snider and Dawson [26], who detected CH_3CN at ground level by an independent method. The results of these authors are also shown in figure 9. Recently acetonitrile has also been measured by the MPIH group in the tropopause using aircraft-borne active chemical ionization mass spectrometry (ACIMS), a method which we will return to in section 4 [33]. The data of the MPIH group are consistent with the results of Snider and Dawson and the estimation for the upper limit of acetonitrile mixing

ratios, deduced by Muller [34] from infrared spectra, obtained at Kitt Peak Observatory and allowing the deduction of trace gas concentrations through absorption techniques. In order to explain the mixing ratio profile of figure 9 some modelling efforts have been made at our institute [35-36]. Two typical results of these theoretical investigations are represented in figure 9 by curves 1 and 2. The major difference between both curves is that for the main destruction process for CH_3CN, i.e. the reaction with hydroxyl radicals, reaction rate coefficients were used from different laboratory measurements [37-39]. The yearly global emission rates (the quantity of material released over the whole Earth per year) required to fit the theoretical curves to the experimental data (0.244 megatons for curve 1 and 0.094 megatons for curve 2) are in reasonable agreement with estimations of the releases from possible sources, such as car exhaust gases, direct releases from industry and biomass burning (wood fires a.s.o.) (36].

As noticed in figure 9, the agreement between theory and experiment is not very satisfactory below 25 km altitude. The reason has recently been discovered and it is due to experimental problems. Laboratory and in flight tests [37, 40] have indeed shown that when the pressure surrounding the mass spectrometer is above a certain value (which is the case below 25 km), the sampled ions undergo too many collisions in the jet expansion region just behind the sampling hole. Due to the accelerating fields of the ion lens some of these collisions are so energetic that the ions are breaking up into different fragments. Such break up effects may result in the loss of a CH_3CN molecule and some NPH ions are reconverted to PH ions, thus falsifying the NPH/PH ratio to be used in equation (8). Preliminary laboratory data [37] indicate that the correction for these electric field induced collisional dissociation effects are of the right order of magnitude to explain the discrepancies observed in figure 9.

3.2. Negative ions

The first stratospheric negative ion composition data, were obtained with a balloon-borne instrument by Arnold and Henschen [41]. They showed that the 2 major ion families are :

1) $NO_3^-.(HNO_3)_n$ cluster ions as predicted by laboratory data [42] and the reaction scheme shown in figure 3 and

2) ions of the type $R^-(HR)_\ell(HNO_3)_m$.

Arnold and Henschen [41] proposed that the latter group of ions originated from reactions of $NO_3^-.(HNO_3)_n$ ions with sulfuric acid vapour. This gas is indeed, formed in the stratosphere through photochemical oxidation of SO_2 as suggested by Turco et al. [43]. The rate constants of the reactions,

$$NO_3^-(HNO_3)_n + H_2SO_4 \rightarrow HSO_4^-(HNO_3)_n + HNO_3 \qquad (11)$$

were subsequently measured in the laboratory by Viggiano et al. [44,45]. Reaction rates of 2.6×10^{-9}, 2.3×10^{-9} and 1.1×10^{-9} cm^3 s^{-1} were found for n = 0,1 and 2 respectively.

In 1980, Arijs et al. [46] measured the first high resolution spectra of negative ions around 35 km. A typical negative ion spectrum is given in figure 10. These measurements allowed an unambiguous mass determination of the major ions and confirmed the H_2SO_4 hypothesis. Negative ion spectra have now been obtained in the altitude range from 20 to 45 km [47-59]. They all showed that the major ions over the whole altitude region were NO_3^- and HSO_4^- core ions. Variations with altitude of ion fractional abundances are caused by variations in sulfuric acid concentration in the stratosphere.

By using a similar steady state treatment as for positive ions, the number density of sulfuric acid converting NO_3^- core ions into HSO_4^- core ions can again be deduced from

$$k_2[n_N]\,[H_2SO_4] = \alpha\,[n^+]\,[n_S] \qquad (12)$$

where $[n^+]$ is the total positive ions density, $[H_2SO_4]$ the sulfuric acid number density, k_2 the rate coefficient of reaction (11) and $[n_S]$ and $[n_N]$ the total number density of HSO_4^- and NO_3^- clusters respectively. A compilation of recent results obtained in this way is given in figure 11. The number densities shown in this figure suffer from large errors due to uncertainties in the values of α, $[n^+]$ and k_2 and due to uncertain $[n_S]$ values, resulting from poor signal strength at lower altitudes. In view of these uncertainties and possible errors on altitude measurements, the data from different sources are in reasonable agreement.

Some recent model calculations for $[H_2SO_4]$ by Turco et al. [60], represented by curves A, B, C and D (full lines above 30 km and dashed lines below) are also shown in figure 11. The dot-and-dash line G is a model result for $[HSO_3]$ [43]. Curves E and F are summations of G + A and G + B (or C, or D) respectively. The dashed line H is a vapour pressure calculation of H_2SO_4 as explained in detail before [56].

The agreement between curve H and the measurements in the altitude region from about 28 to 33 km suggests that in this region the H_2SO_4 number density is controlled by the evaporation-recondensation equilibrium of aerosol droplets. Below 28 km, the H_2SO_4 vapour is clearly in supersaturation, suggesting that the liquid-vapour equilibrium is disturbed by the oxidation of SO_2 vapour through the reactions

$$SO_2 + OH + M \rightarrow HSO_3 + M \quad (13)$$

$$HSO_3 + O_2 \rightarrow SO_3 + HO_2 \quad (14)$$

and

$$SO_3 + H_2O \rightarrow H_2SO_4 \quad (15)$$

The main loss processes for sulfuric acid vapour are interaction with aerosols. Above 35 km, the measurements seem to suggest a good agreement with curve B, obtained by assuming a loss of H_2SO_4 by reaction with "smoke" particles, caused by a downward metal flux of 10^6 cm^2 s^{-1} from meteoric debris [60].

Nitric acid is another important trace gas in the stratosphere. And its concentration can also be derived from negative ion composition data. Apart from the steady state method [48, 49, 53] explained in the previous paragraphs for CH_3CN and H_2SO_4, another technique, called the equilibrium method [50, 61] can be applied here. This method is based on the fact that the number density ratio of two cluster ions from the same family such as $NO_3^-(HNO_3)$ and $NO_3^-(HNO_3)_2$ is given by :

$$\frac{[NO_3^-(HNO_3)_2]}{[NO_3^-.HNO_3]} = K.p(HNO_3) \quad (16)$$

where square brackets denote number densities, K is the equilibrium constant and $p(HNO_3)$ is the partial pressure of nitric acid vapour.

Since K can be deduced from laboratory measurements, $p(HNO_3)$ can be derived from the ratio of the peak intensities as observed at mass 188 and 125 in the ion spectra.

The data derived in this way from the ion spectra, obtained at different altitudes, are shown in figure 12. In the same figure, these results are compared to model calculations and experimental data obtained by other (mostly optical) methods [62]. As can be seen, above 30 km the agreement with our data is reasonable. Below this altitude however the HNO_3 mixing ratios inferred from ion spectra are much too low. The reason for this is cluster break up in the mass spectrometer which results in the conversion of $NO_3^-(HNO_3)_2$ clusters into $NO_3^-.HNO_3$ ions, thus falsifying the abundance ratio to be used in formula (16) [63].

4. CONCLUSIVE REMARKS AND FUTURE PERSPECTIVES

In the previous paragraph, it has been shown that from the spectra of natural ions obtained hitherto, the concentration of at least three kind of trace gases can be derived, namely CH_3CN, H_2SO_4 and HNO_3. Although acetonitrile does not play an important role in any of the major atmospheric cycles, some attention has been paid to it, merely to obtain a consistent picture of the positive stratospheric ion density [36-37].

Sulfuric acid however is a much more important trace gas since it is the precursor of aerosols, which in the stratosphere consist of microscopic droplets of water and H_2SO_4 and may have an impact on the Earth's radiation budget and thus on our climate. Nitric acid is one of the major gases of the NO_x group, which actively participate in the ozone cycle.

So far only the major mass peaks of ion spectra have been used for the derivation of trace gas profiles. An investigation of the lower part of figure 3 however shows that the minor mass peaks can be assigned to the action of some other trace gases. For instance, the mass peaks at 33 and 51 amu are most probably due to protonated methanol clusters $[H^+.CH_3OH(H_2O)_n]$. Also negative ion mass spectra show several smaller peaks [50], which are due to gases so far not detected. It is evident that if much more sensitive ion mass spectrometers could be developed, a wealth of information might be inferred from ion mass spectrometry. Presently however the method for derivation of trace gases from the spectra of natural ions suffers from some drawbaks, which are :

1. The method is limited to those gases which intervene in the final stages of the ion-molecule reaction chain leading to the terminal ions.
2. Cluster break up of the sampled ions, just behind the sampling hole can lead to falsified results (e.g. NPH to PH reconversion) and should be studied more intensively before using new results of more sensitive instruments.
3. The exploitation of ion mass spectra strongly depends upon the availability of laboratory data, such as reaction rate constants of appropriate ion molecule reactions and thermochemical data. Therefore laboratory studies should be performed in parallel with the in-situ measurements.

Recently the group of the Max-Planck-Institut für Kernphysik of Heidelberg has developed a new method for the derivation of trace gases from ion mass spectrometry, which they have called ACIMS (active chemical ionization mass spectrometry) [64]. In this method an active ion source is added to the instrument and the ions formed in the atmo-

sphere are conducted to the mass spectrometer through a flow tube, activated by a small turbine. This method has some distinct advantages, such as enhanced ionization and thus higher signal of ions with a smaller lifetime than the natural ions (the lifetime in this case is simply the time of flight in the flow tube). Due to this reduced lifetime trace gases which intervene in the intermediate stages of the ion-chemistry may be deduced more easily.

This technique is rather promising because a number of variations are possible in the future, such as selective ion sources (producing ions which selectively react with some trace gases). At present the research in our institute is directed towards that direction.

REFERENCES

1. OPPENHEIMER, M., CONSTANTINIDES, E.R., KIRBY-DOCKEN, K., VICTOR, G.A., DALGARNO, A. and HOFFMAN, J.H., J. Geophys. Res., 82, 5485, 1977.
2. KENESHEA, T.J., NARCISI, R.S. and SWIDER, W.J., J. Geophys. Res., 75, 845, 1970.
3. NICOLET, M. and AIKIN, A.C., J. Geophys. Res., 65, 5, 1960.
4. NARCISI, R.S. and BAILEY, A.D., J. Geophys. Res., 70, 3687, 1965.
5. GOLDBERG, R.A. and AIKIN, A.C., J. Geophys. Res., 76, 8352, 1971.
6. NARCISI, R.S., BAILEY, A.D., WLODYKA, L.E. and PHILBRICK, C.R., J. Atmos. Terr. Phys., 34, 647, 1972.
7. REID, C.G., Adv. At. Mol. Phys., 63, 375, 1976.
8. FEHSENFELD, F.C. and FERGUSON, E.E., J. Geophys. Res., 74, 2217, 1969.
9. FERGUSON, E.E., in Gas Phase Ion Chemistry, ed. M.T. Bowers (Academic Press), pp. 45-82, 1979.
10. ARNOLD, F., KISSEL, J., KRANKOWSKY, D., WIEDER, H. and ZAEHRINGER, J., J. Atmos. Terr. Phys., 33, 1169, 1971.
11. NARCISI, R.S., BAILEY, A.D., DELLA LUCCA, L., SHERMAN, C. and THOMAS, D.M., J. Atmos. Terr. Phys., 33, 1147, 1971.
12. NEHER, H.V., J. Geophys. Res., 72, 1527, 1967.
13. SMITH, D. and ADAMS, N.G., Geophys. Res. Lett., 9, 1085, 1982.
14. INGELS, J., ARIJS, E., NEVEJANS, D., FORTH, H.J. and SCHAEFFER, G., Rev. Sci. Instr., 49, 782, 1978.
15. NEVEJANS, D., INGELS, J. and ARIJS, E., in "Handbook for MAP - volume 15 - Balloon Techniques", ed. D.G. Murcray, pp. 124-138, 1985.
16. NEVEJANS, D., FREDERICK, P. and ARIJS, E., Bull. Ac. Roy. Belg. Cl. Sci., 67, 314, 1982.
17. ARNOLD, F., ESA-PAC Symposium on European Rocket and Balloon Program, Bournemouth, ed. ESA, pp. 479-496, 1980.
18. ARIJS, E., Annales Geophysicae, 1, 149, 1983.

19. ARIJS, E., Adv. Space Res., 4, 19, 1984.
20. ARIJS, E., INGELS, J. and NEVEJANS, D., Nature, 271, 642, 1978.
21. ARIJS, E., NEVEJANS, D. and INGELS, J., Nature, 288, 684, 1980.
22. ARNOLD, F., BOEHRINGER, H. and HENSCHEN, G., Geophys. Res. Lett., 5 653, 1978.
23. ARNOLD, F., HENSCHEN, G. and FERGUSON, E.E., Planet. Space Sci., 29, 185, 1981.
24. SMITH, D., ADAMS, N.G. and ALGE, E., Planet. Space Sci., 29, 449, 1981.
25. BOEHRINGER, H. and ARNOLD, F., Nature, 290, 321, 1981.
26. SNIDER, J.R. and DAWSON, G.A., Geophys. Res. Lett., 11, 241, 1984.
27. SCHLAGER, H. and ARNOLD, F., Planet. Space Sci., 33, 1363, 1985.
28. ROSEN, J.M. and HOFMAN, D.J., J. Geophys. Res., 86, 7399, 1981.
29. ARIJS, E., INGELS, J., NEVEJANS, D. and FREDERICK, P., Annales Geophysicae, 1, 161, 1983.
30. BATES, D.R., Planet. Space Sci., 30, 1275, 1982.
31. ROSEN, J.M. and HOFMANN, D.J., J. Geophys. Res., 86, 7406, 1981.
32. HEAPS, M.G., Planet. Space Sci., 26, 513, 1978.
33. KNOP, G. and ARNOLD, F., Planet. Space Sci., 35, 259, 1987.
34. MULLER, C., Bull. Ac. Roy. Belg. Cl. Sci., 71, 225, 1985.
35. BRASSEUR, G., ARIJS, E., DE RUDDER, A., NEVEJANS, D. and INGELS, J., Geophys. Res. Lett., 12, 117, 1985.
36. ARIJS, E. and BRASSEUR, G., J. Geophys. Res., 91, 4003, 1986.
37. ARIJS, E., NEVEJANS, D. and INGELS, J., Int. J. Mass Spect. Ion Processes, 81, 15, 1987.
38. HARRIS, G.W., KLEINDIENST, T.E. and PITTS, J.N. Jr., Chem. Phys. Lett., 80, 479, 1981.
39. KURYLO, M.G. and KNABLE, G.M., J. Phys. Chem., 88, 3305, 1984.
40. SCHLAGER, H. and ARNOLD, F., Planet. Space Sci., 35, 715, 1987.
41. ARNOLD, F. and HENSCHEN, G., Nature, 275, 521, 1978.
42. FEHSENFELD, F.C., HOWARD, C.J. and SCHMELTEKOPF, A.L., J. Chem. Phys., 63, 2835, 1975.
43. TURCO, R.P., HAMILL, P., TOON, O.B., WHITTEN, R.C. and KIANG, C.S., J. Atm. Sci., 36, 699, 1979.
44. VIGGIANO, A.A., PERRY, R.A., ALBRITTON, D.L., FERGUSON, E.E. and FEHSENFELD, F.C., J. Geophys. Res., 85, 4551, 1980.
45. VIGGIANO, A.A., PERRY, R.A., ALBRITTON, D.L., FERGUSON, E.E. and FEHSENFELD, F.C., J. Geophys. Res., 87, 7340, 1982.
46. ARIJS, E., NEVEJANS, D., FREDERICK, P. and INGELS, J., Geophys. Res. Lett., 8, 121, 1981.
47. ARNOLD, F., FABIAN, R., FERGUSON, E.E. and JOOS, W., Planet. Space Sci., 29, 195, 1981.
48. VIGGIANO, A.A. and ARNOLD, F., Planet. Space Sci., 29, 895, 1981.
49. McCRUMB, J.L. and ARNOLD, F., Nature, 294, 136, 1981.

50. ARIJS, E., NEVEJANS, D., FREDERICK, P. and INGELS, J., J. Atmos. Terr. Phys., 44, 681, 1982.
51. VIGGIANO, A.A., SCHLAGER, H. and ARNOLD, F., Planet. Space Sci., 31, 813, 1983.
52. ARIJS, E., NEVEJANS, D., INGELS, J. and FREDERICK, P., Planet. Space Sci., 31, 1459, 1983.
53. ARNOLD, F. and QIU, S., Planet. Space Sci., 32, 169, 1984.
54. ARNOLD, F. and FABIAN, R., Nature, 283, 55, 1980.
55. ARNOLD, F., FABIAN, R. and JOOS, W., Geophys. Res. Lett., 8, 293, 1981.
56. ARIJS, E., NEVEJANS, D., INGELS, J. and FREDERICK, P., Geophys. Res. Lett., 10, 329, 1983.
57. VIGGIANO, A.A. and ARNOLD, F., Geophys. Res. Lett., 8, 583, 1981.
58. VIGGIANO, A.A. and ARNOLD, F., J. Geophys. Res., 88, 1457, 1983.
59. QIU, S. and ARNOLD, F., Planet. Space Sci., 32, 87, 1984.
60. TURCO, R.P., TOON, O.B., HAMILL, P. and WHITTEN, R.C., J. Geophys. Res., 86, 1113, 1981.
61. ARNOLD, F., FABIAN, R., HENSCHEN, G. and JOOS, W., Planet. Space Sci., 28, 681, 1980.
62. W.M.O. Report n° 11, pages 1-98 and 1-152, 1981.
63. ARIJS, E., NEVEJANS, D., INGELS, J. and FREDERICK, P., J. Geophys. Res., 90, 5891, 1985.
64. ARNOLD, F. and KNOP, G., Int. J. Mass Spectr. and Ion Processes, 81, 133, 1987.

TABLE 1 : Major positive ions as observed by the first in situ mass spectrometer measurements at typical balloon float altitudes (35-37 km).

Mass in amu		Proposed ion clusters
(1)	(2)	
20 ± 3		$H^+(H_2O)$
29 ± 3		?
37 ± 3		$H^+(H_2O)_2$
43 ± 3		H^+X
50 ± 3		?
55 ± 3	55	$H^+(H_2O)_3$
60 ± 2		$H^+X(H_2O)$
73 ± 2	73 ± 1	$H^+X(H_2O)_2$
82 ± 2	78 ± 2	H^+X_2
91 ± 2	91 ± 1	$H^+(H_2O)_5$
96 ± 2	96 ± 1	$H^+X(H_2O)_3$
99 ± 2	100 ± 1	$H^+X_2(H_2O)$
109 ± 2		$H^+(H_2O)_6$
	114 ± 2	$H^+X(H_2O)_4$
	118 ± 1	$H^+X_2(H_2O)_2$
	136 ± 2	$H^+X_2(H_2O)_3$
	140 ± 2	$H^+X_3(H_2O)$

(1) Ref. [20]
(2) Ref. [22]
$X \equiv CH_3CN$

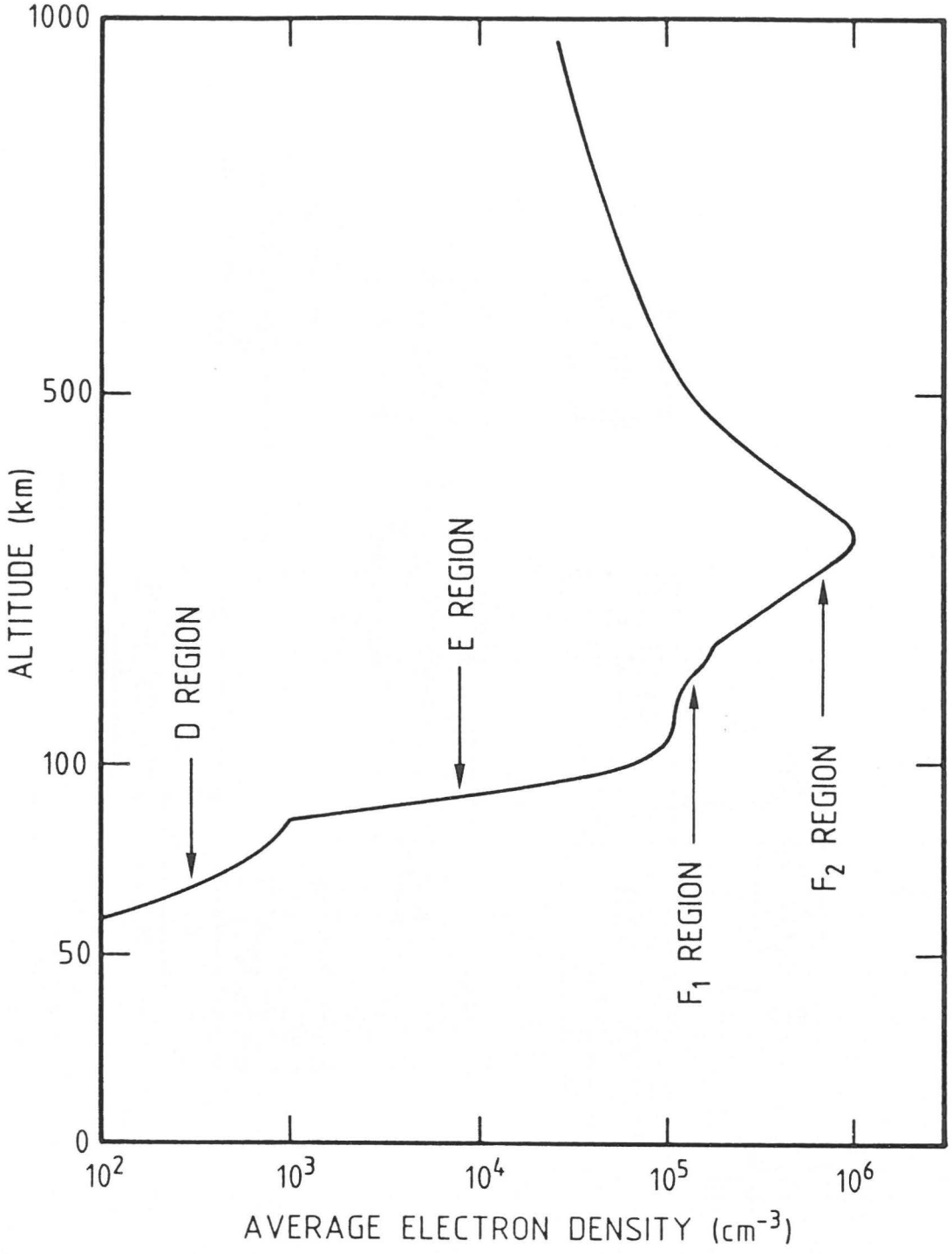

Figure 1
Different layers of the ionosphere, as defined by the average electron density versus altitude.

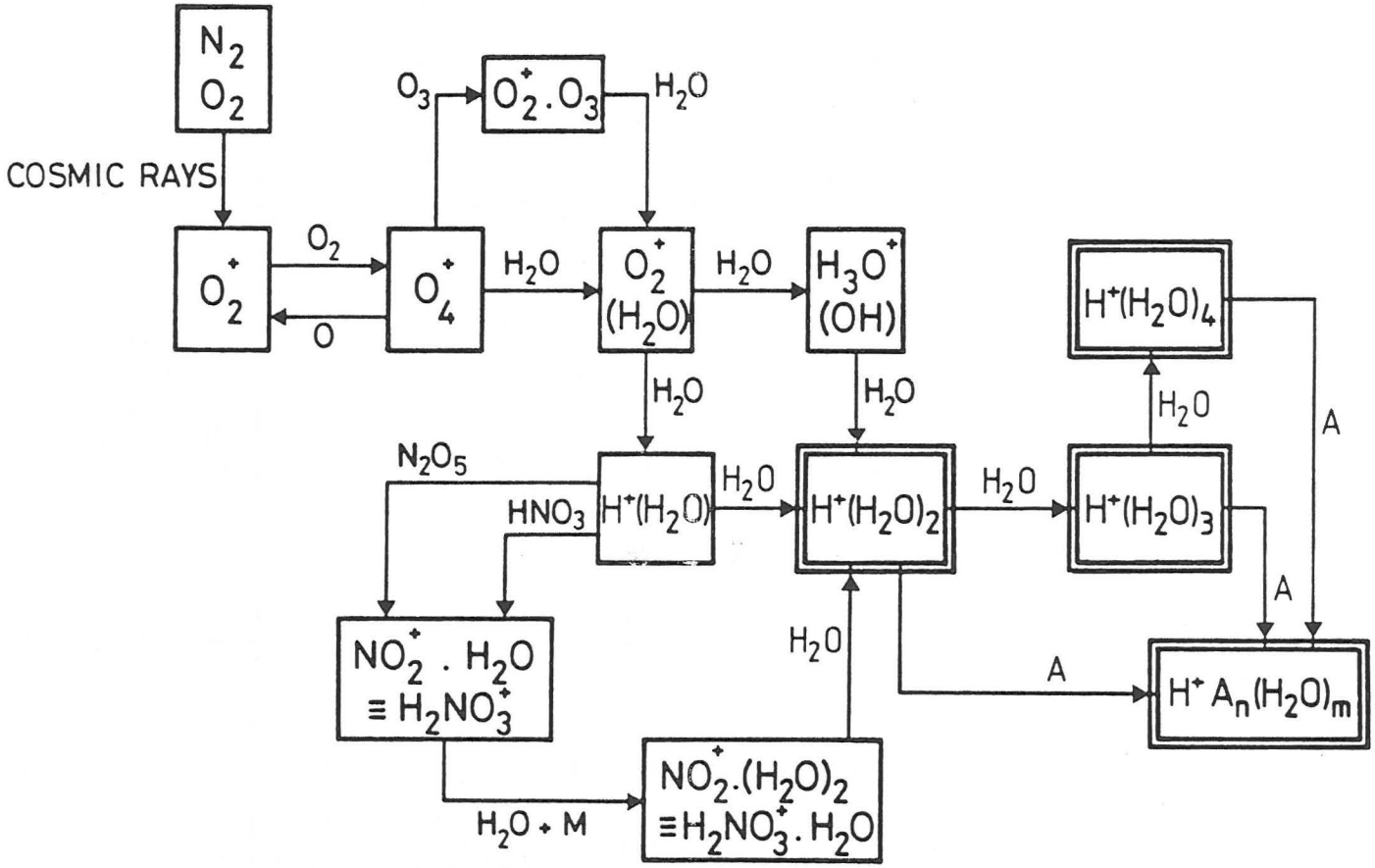

Figure 2

Reaction scheme leading to the terminal positive ions in the stratosphere.

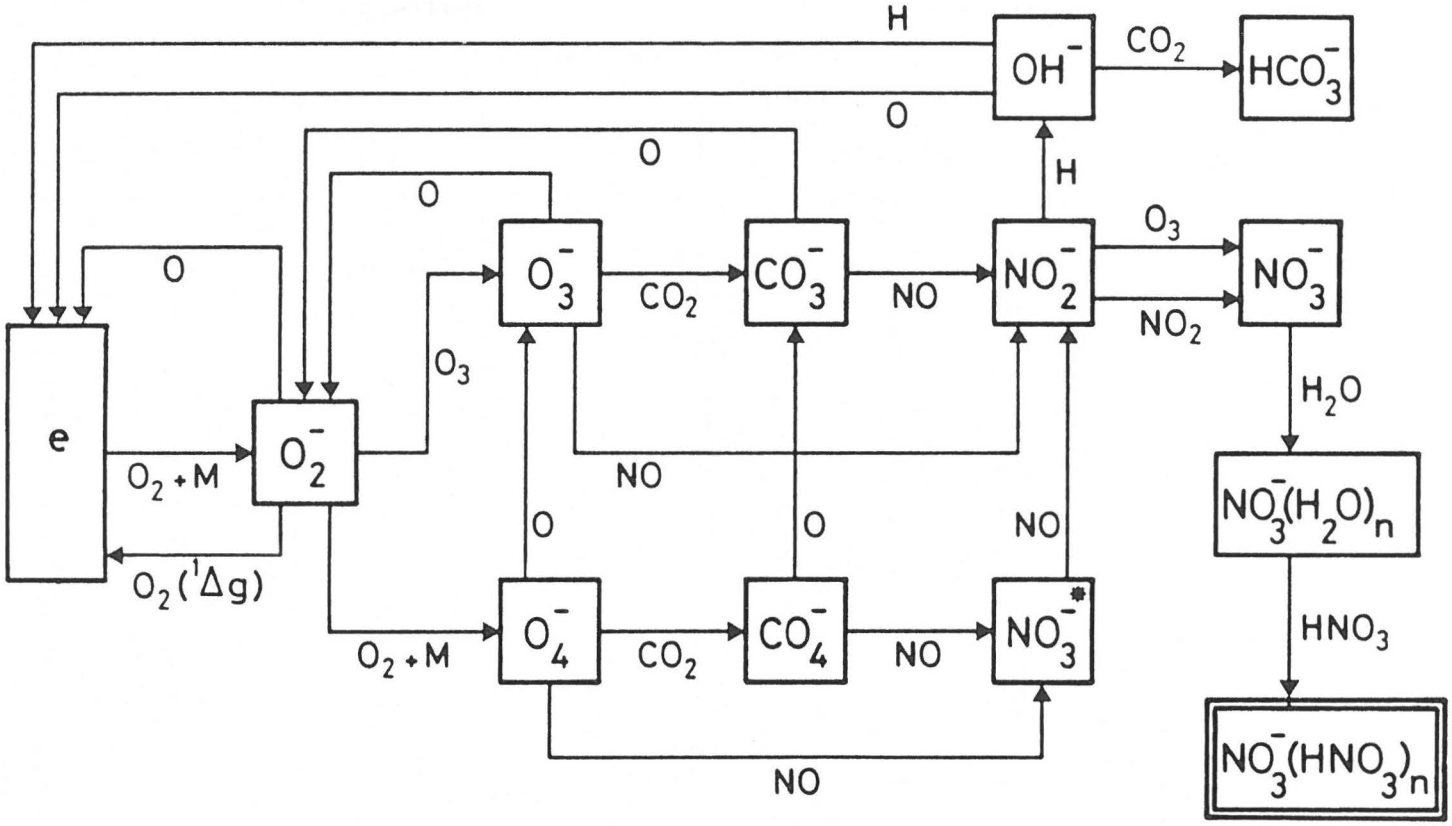

Figure 3

Stratospheric negative ion reaction scheme adapted from Ferguson, Ion Chemistry of the normal earth's stratosphere : The natural stratosphere, CIAP monograph 1, page 5.42-5.54.

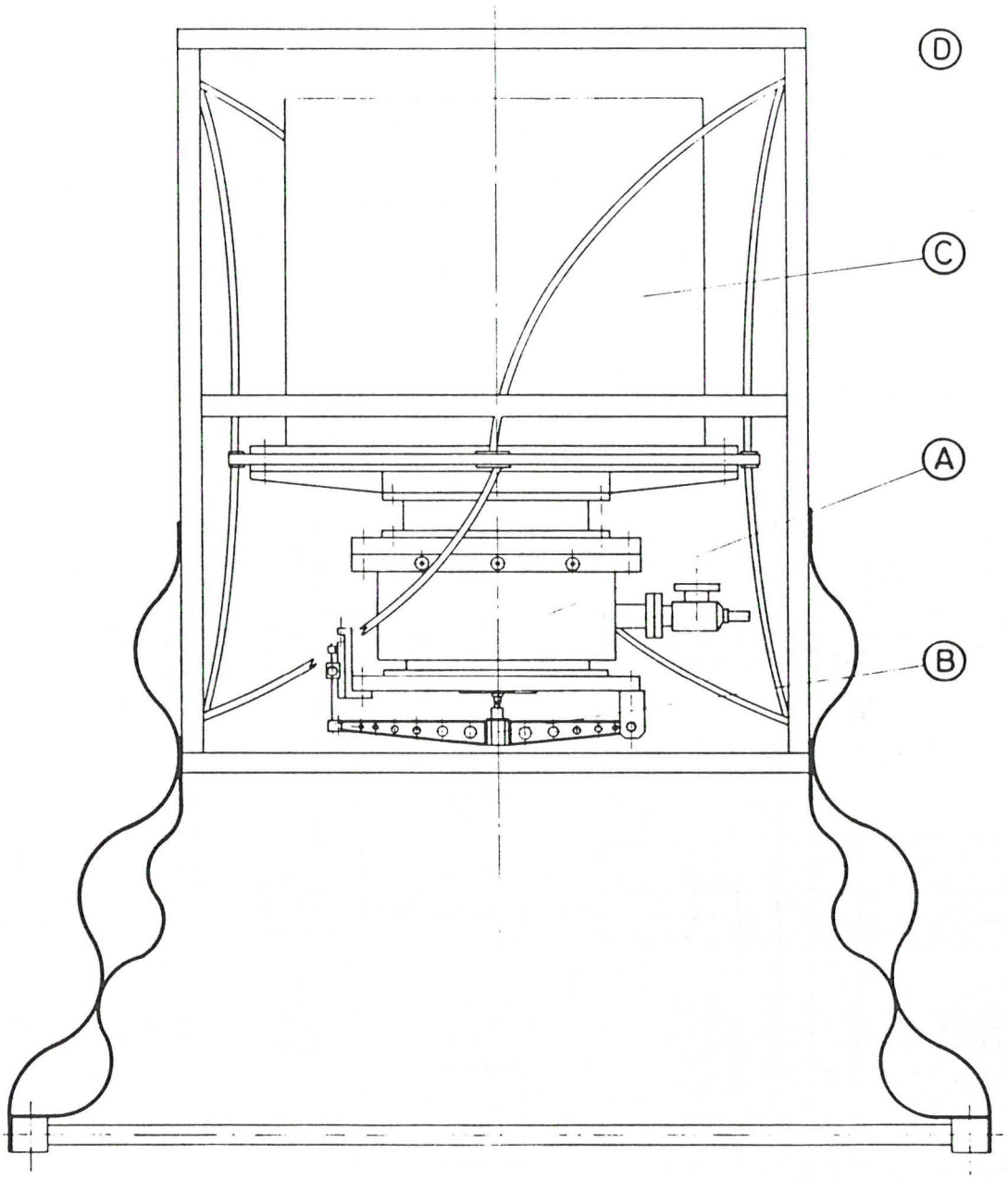

Figure 4
Schematic general view of balloon gondola element for ion mass spectrometer. A : Cryopump; B : opening device; C : electronics container; D : mechanical support structure.

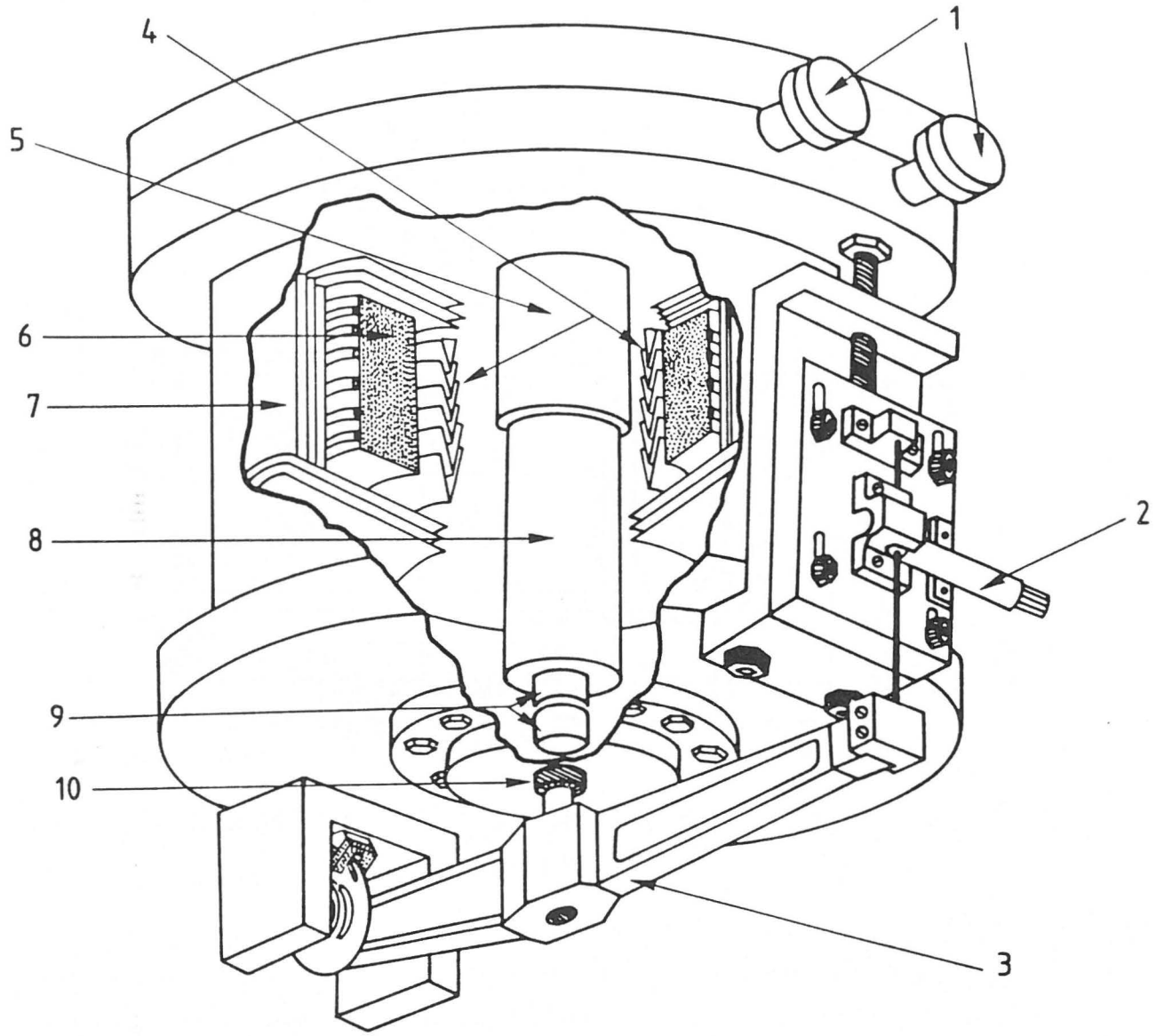

Figure 5

Sketch of high vacuum part of the BISA ion mass spectrometer. 1 : liquid helium in-and output; 2 : Pyrotechnical cable cutter; 3 : opening device; 4 : Chevron baffles for liquid helium container; 5 : electron multiplier housing; 6 : liquid helium reservoir; 7 : Thermal superinsulation; 8 : Quadrupole; 9 : ion lens.

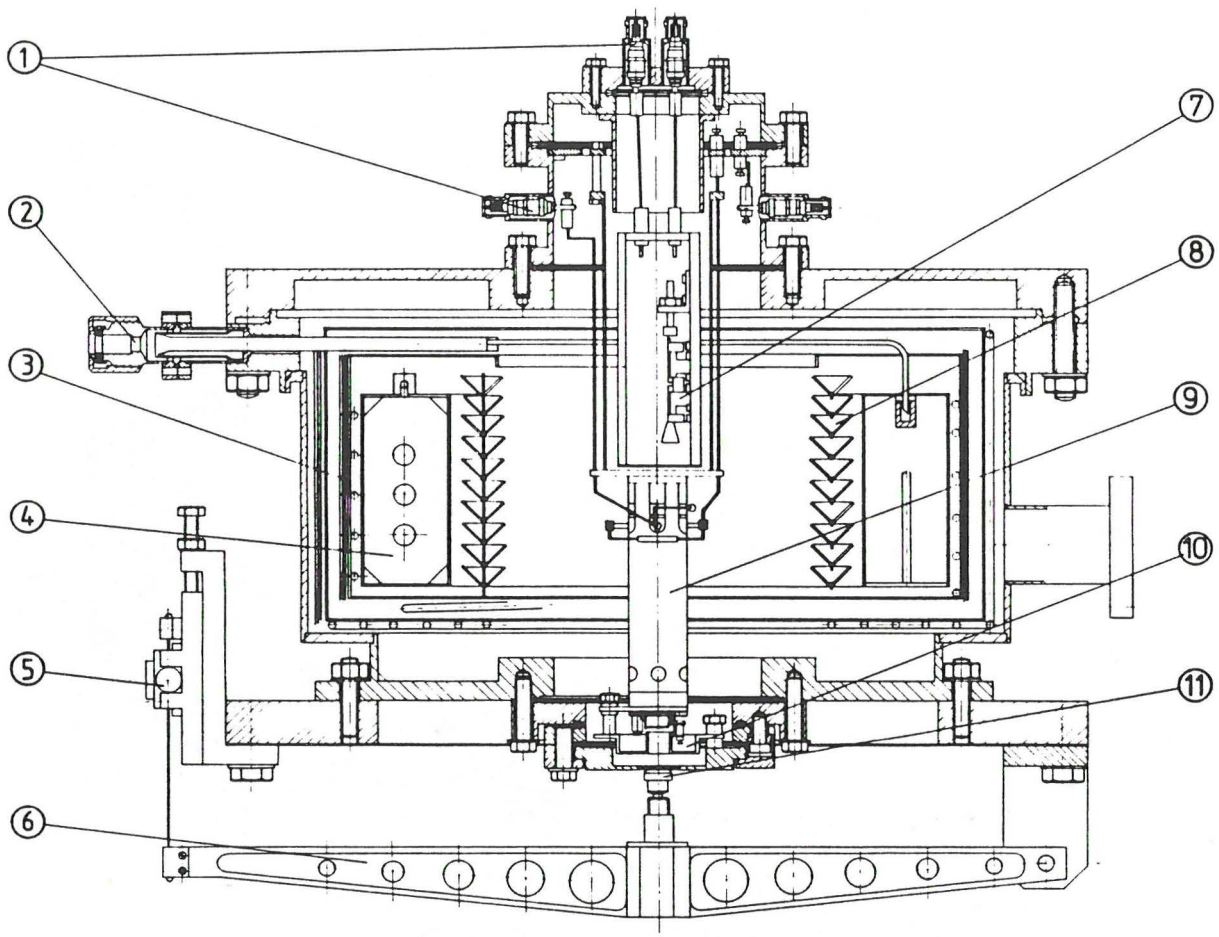

Figure 6

Detailed view of high vacuum part of ion mass spectrometer; 1 : electrical feedthroughs; 2 : liquid helium inlet; 3 : Superinsulation; 4 : Liquid heliumreservoir; 5 : Cable cutter; 6 : Opening device; 7 : Electron multiplier (Spiraltron); 8 : Chevron baffles; 9 : Quadrupole; 10 : Ion lens; 11 : Polyimide plunger.

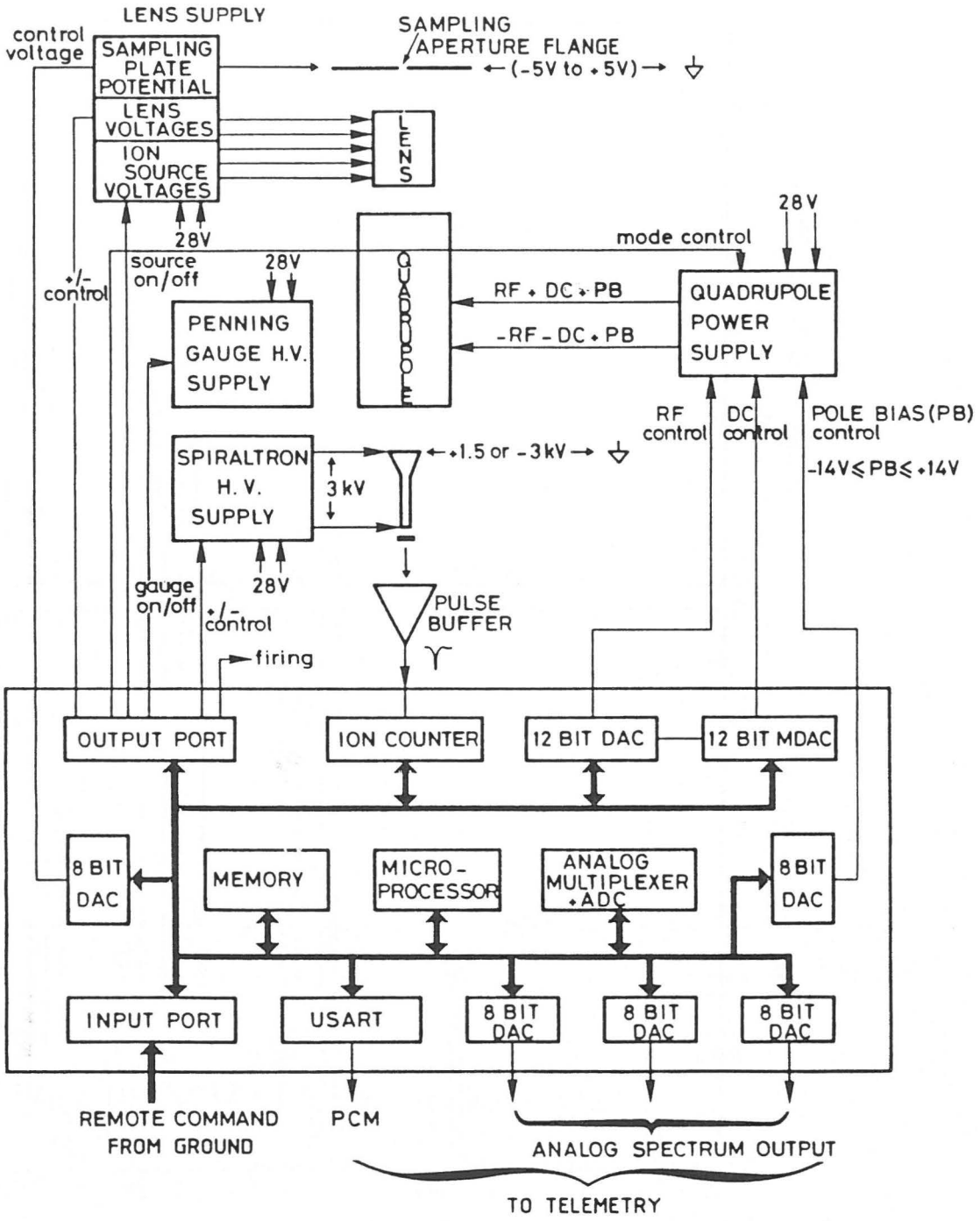

Figure 7

Block diagram of balloon borne electronics for BISA ion mass spectrometer.

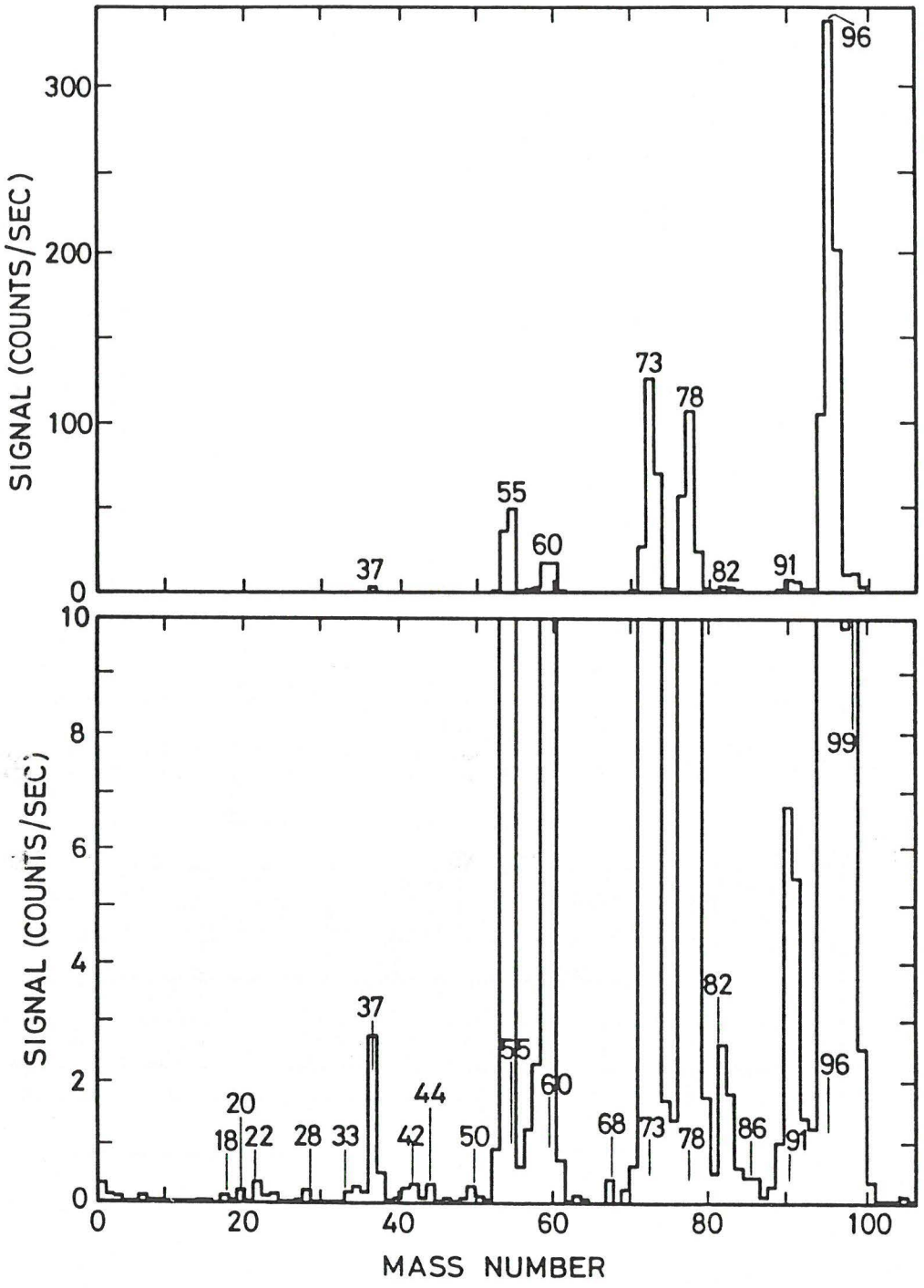

Figure 8

Typical positive ion mass spectrum obtained at 35 km altitude. Lower figure is the enlarged version of upper spectrum.

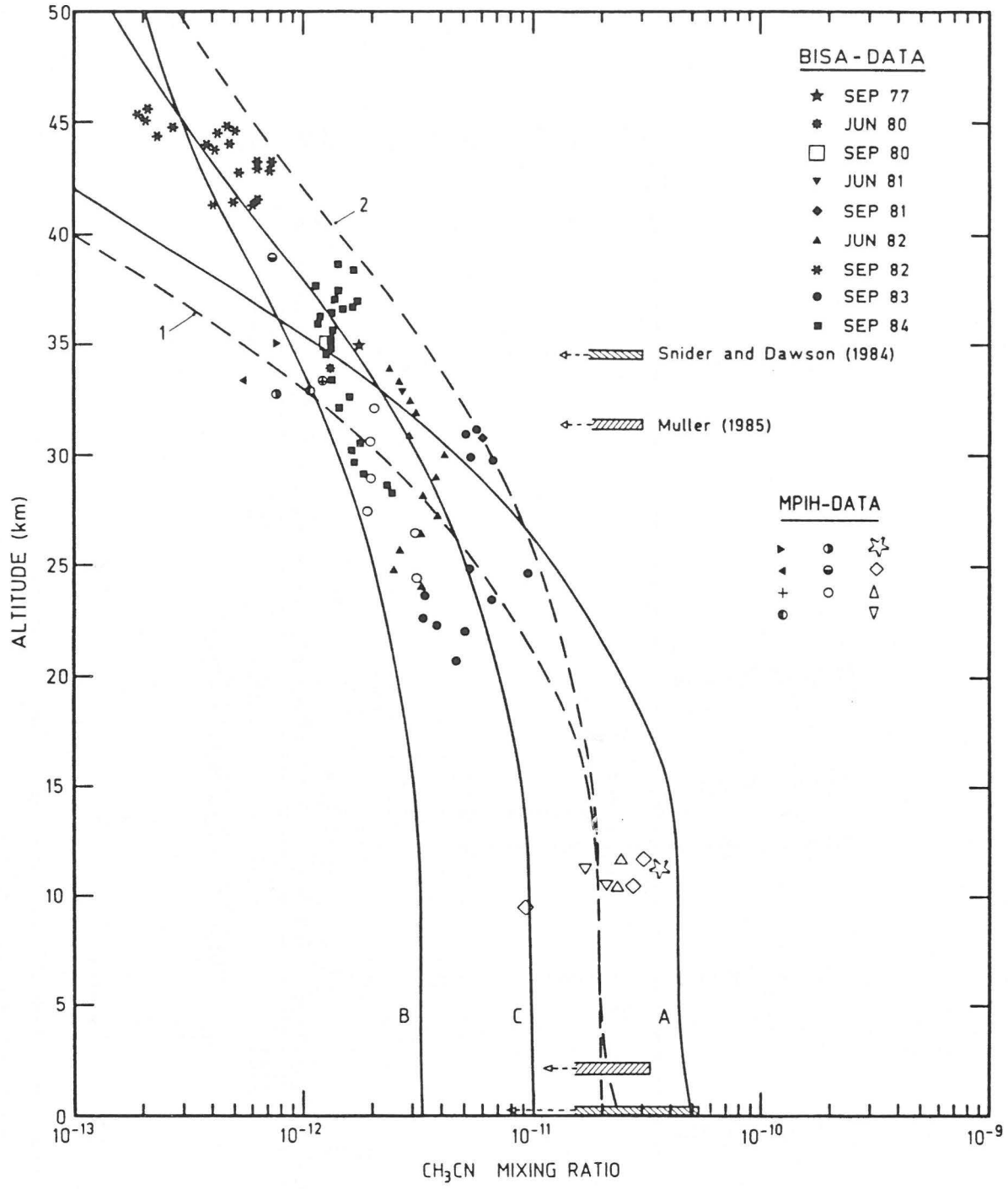

Figure 9

Acetonitrile mixing ratio profile as derived from positive ion spectra (altitudes above 20 km), from ACIMS measurements with airplanes (around 10 km), from optical data (at 2 km) and from in-situ ground level measurements. The full and dotted line curves are model calculations.

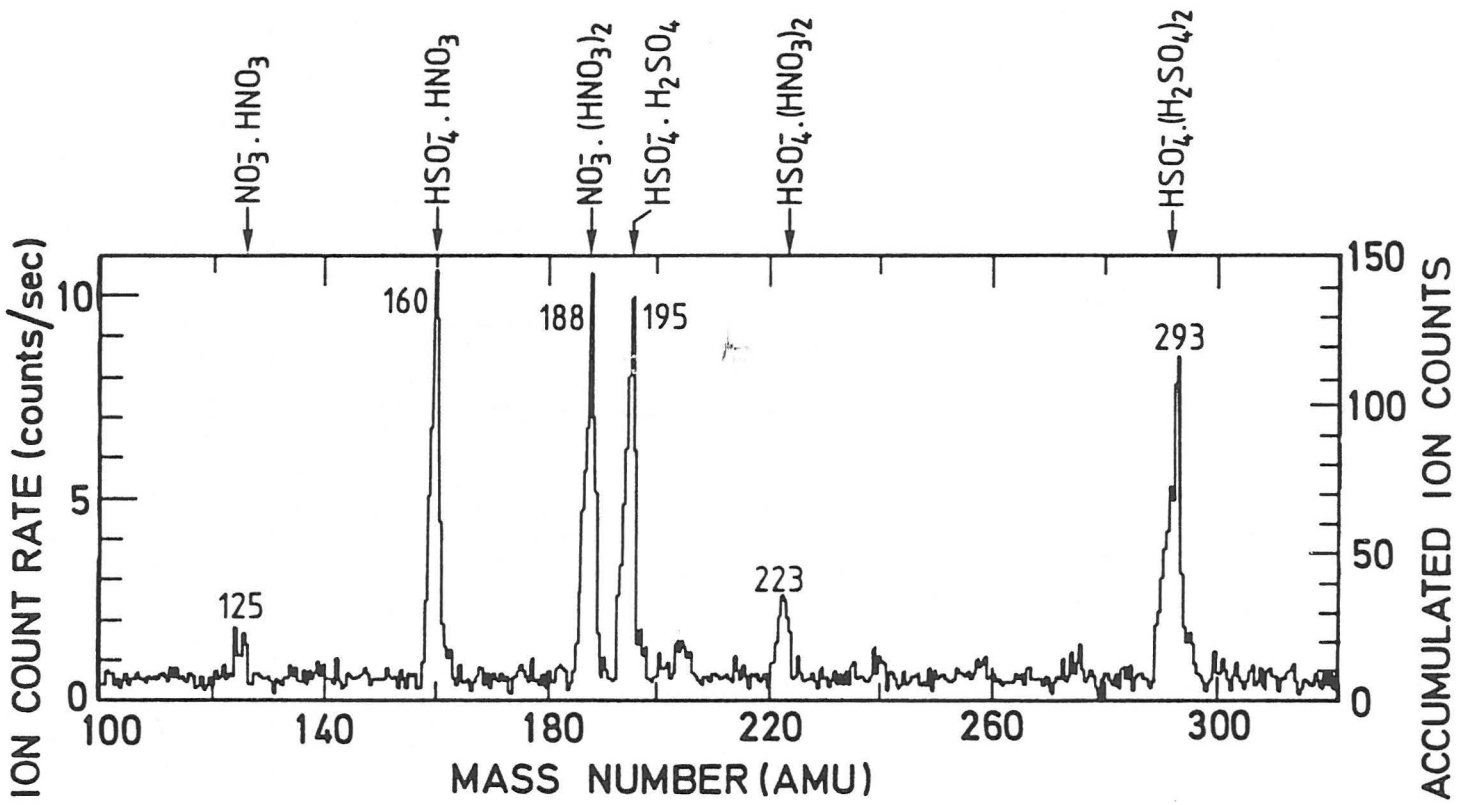

Figure 10

Typical negative ion spectrum obtained around 35 km. Mass numbers and identification for major mass peaks are also shown.

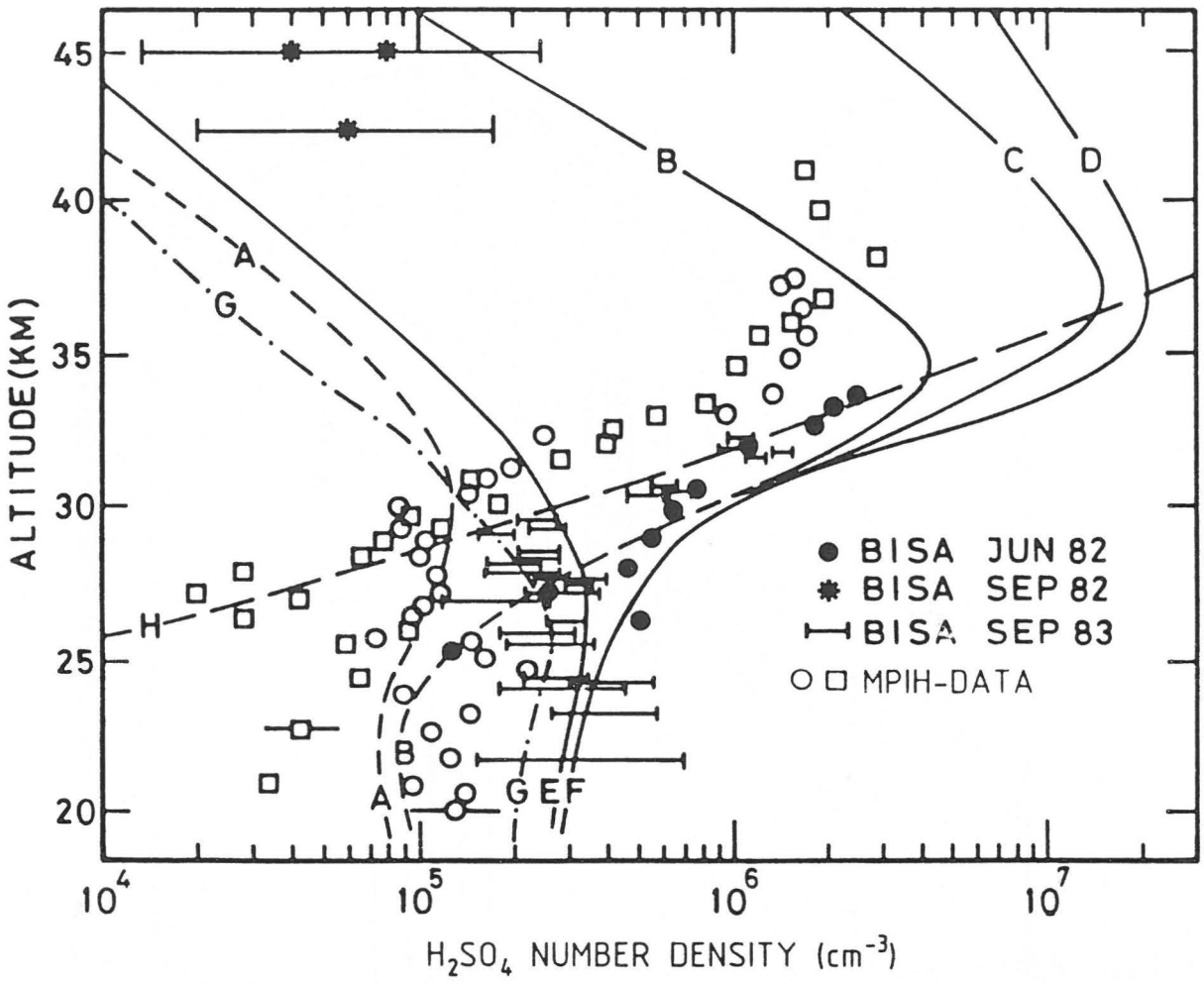

Figure 11
Sulfuric acid vapour concentrations versus altitude as derived from negative ion mass spectra, compared to model calculations.

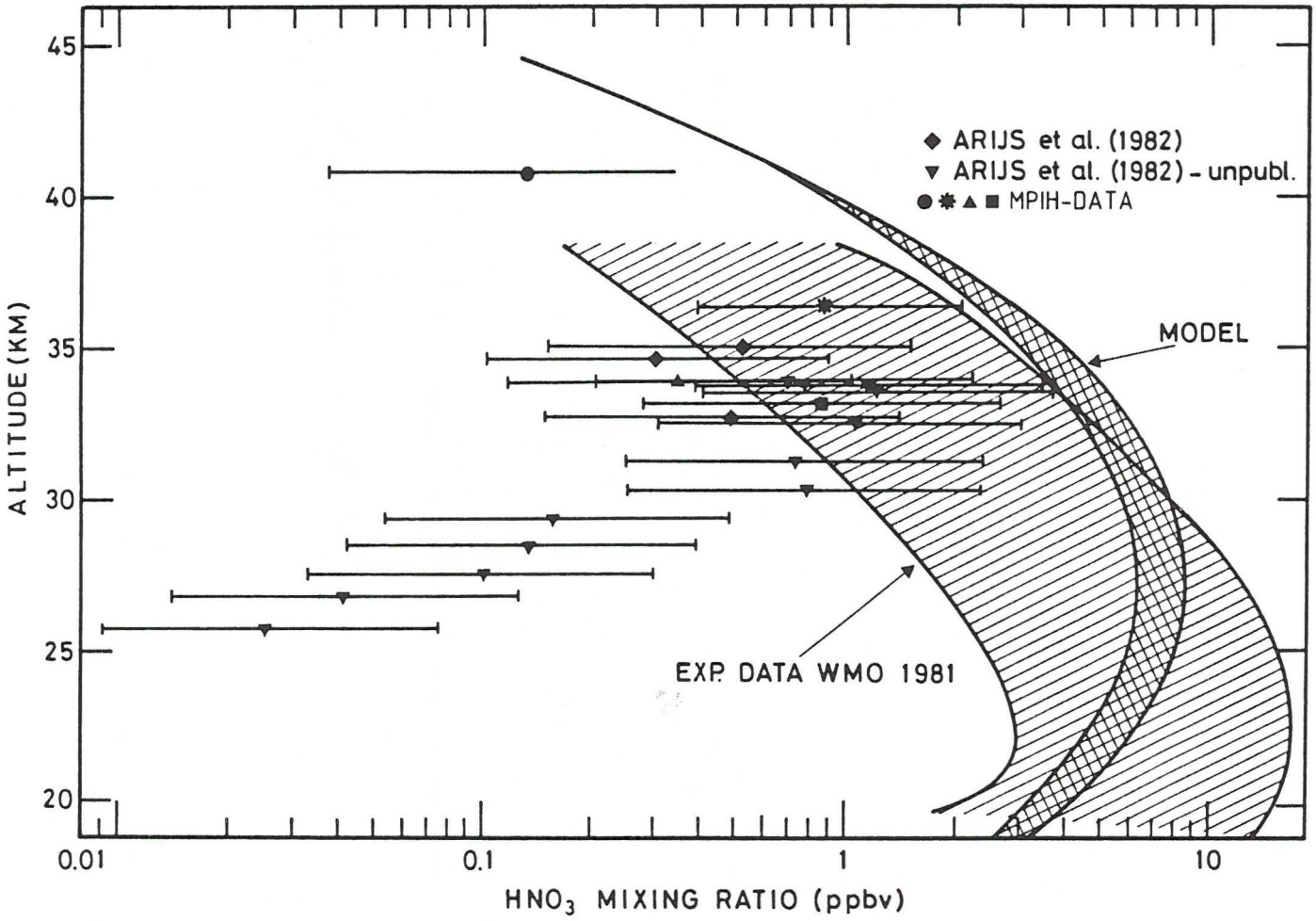

Figure 12

Comparison between nitric acid vapour mixing ratios inferred from negative ion spectra with other measurements and model calculations.